

1 **Recent evolution and associated hydrological dynamics of a vanishing tropical Andean**
2 **glacier: *Glaciar de Conejeras*, Colombia**

3
4 Enrique Morán-Tejeda¹, Jorge Luis Ceballos², Katherine Peña², Jorge Lorenzo-Lacruz¹ and
5 Juan Ignacio López-Moreno³

- 6
7 1. Department of Geography. University of the Balearic Islands. Palma, Spain
8 2. Instituto de Hidrología, Meteorología y Estudios Ambientales (IDEAM). Bogotá, Colombia
9 3. Pyrenean Institute of Ecology. Consejo Superior de Investigaciones Científicas. Zaragoza, Spain.

10
11
12 **Abstract**

13 Glaciers in the inner tropics are rapidly retreating due to atmospheric warming. In Colombia, this
14 retreat is accelerated by volcanic activity, and most glaciers are in their last stages of existence.
15 There is general concern about the hydrological implications of receding glaciers, as they
16 constitute important freshwater reservoirs and, after an initial increase in melting flows due to
17 glacier retreat, a decrease in water resources is expected in the long term as glaciers become
18 smaller. In this paper, we perform a comprehensive study of the evolution of a small Colombian
19 glacier, Conejeras (Parque Nacional Natural de los Nevados) that has been monitored since
20 2006, with special focus on the hydrological response of the glacierized catchment. The glacier
21 shows great sensitivity to changes in temperature and especially to the evolution of the El Niño
22 Southern Oscillation (ENSO) phenomenon, with great loss of mass and area during El Niño warm
23 events. Since 2006, it has suffered a 37% reduction, from 22.45 ha in 2006 to 12 ha in 2017, with
24 an especially abrupt reduction since 2014. During the period of hydrological monitoring (June
25 2013 to December 2017), streamflow at the outlet of the catchment experienced a noticeable
26 cycle of increasing flows up to mid-2016 and decreasing flows afterwards. The same cycle was
27 observed for other hydrological indicators, including the slope of the rising flow limb and the
28 monthly variability of flows. We observed an evident change in the daily hydrograph, from a
29 predominance of days with a pure melt-driven hydrograph up to mid-2016, to an increase in the
30 frequency of days with flows less influenced by melt after 2016. Such a hydrological cycle is not
31 directly related to fluctuations of temperature or precipitation; therefore, it is reasonable to
32 consider that it is the response of the glacierized catchment to retreat of the glacier. Results
33 confirm the necessity for small-scale studies at a high temporal resolution, in order to understand
34 the hydrological response of glacier-covered catchments to glacier retreat and imminent glacier
35 extinction.

36
37
38 **Key words:** glacier retreat, melting flows, tropical glaciers; hydrological change; tipping point
39
40
41
42
43
44
45
46
47
48

49 **1. Introduction**

50 **1.2 Andean glaciers and water resources**

51 Glacier retreat is one the most prominent signals of global warming; glaciers from most mountain
52 regions in the world are disappearing or have already disappeared due to atmospheric warming
53 (Vaughan et al., 2013). Of the retreating mountain glaciers worldwide, those located within the
54 tropics are particularly sensitive to atmospheric warming (Chevallier et al., 2011; Kaser and
55 Omaston, 2002). Their locations in the tropical region involve a larger energy forcing, in terms of
56 received solar radiation, compared to other latitudes. Unlike glaciers in mid and high latitudes,
57 which are subject to freezing temperatures during a sustained season, tropical glaciers may
58 experience above-zero temperatures all year round, especially at the lowest elevations, involving
59 constant ablation and rapid response of the glacier snout to climate variability and climate change
60 (Francou et al., 2004; Rabatel et al., 2013). As a result of atmospheric warming since the mid-
61 20th century, glaciers in the tropics are seriously threatened, and many of them have already
62 disappeared (Vuille et al., 2008). Of the tropical glaciers, 99% are located in the Central Andes
63 and constitute a laboratory for glaciology (see review in Vuille et al., 2017), including studies of
64 glacier response to climate forcing (e.g. Favier et al., 2004; Francou et al., 2004, 2003; López-
65 Moreno et al., 2014), hydrological and geomorphological consequences of glacier retreat (Bradley
66 et al., 2006; Chevallier et al., 2011; Kaser et al., 2010; López-Moreno et al., 2017; Ribstein et al.,
67 1995; Sicart et al., 2011) and the vulnerability of populations to risks associated with glacier retreat
68 (Mark et al., 2017). Perhaps the glaciers in the most critical situation in the Andean mountains
69 are those located in the inner tropics, including the countries of Ecuador, Venezuela and
70 Colombia (Klein et al., 2006; Rekowski, 2016). In the latter country, a constant glacier recession
71 since the 1970s has been reported, with an acceleration since the 2000s (Ceballos et al., 2006;
72 Rabatel et al., 2013), and most glaciers are in danger of disappearing in the coming years
73 (Poveda and Pineda, 2009; Rabatel et al., 2017). In the outer tropics, the variability of glacier
74 mass balance is highly dependent on seasonal precipitation; thus, during the wet season
75 (December-February), freezing temperatures ensure seasonal snow cover that increases the
76 glaciers' surface albedo and compensates mass balance losses of the dry season. In contrast,
77 for glaciers of the inner tropics, ablation rates remain more or less constant throughout the year
78 due to the absence of seasonal fluctuations of temperature and to a freezing level which is
79 constantly oscillating within the glaciers' elevation ranges. Therefore, the mass balance of these
80 glaciers is more sensitive to inter-annual variations of temperature, and they are much more
81 sensitive to climate warming (Ceballos et al., 2006; Favier et al., 2004; Francou et al., 2004;
82 Rabatel et al., 2013, 2017). In Colombia, this situation is further aggravated by the location of
83 glaciers near or on the top of active volcanos. The hot pyroclastic material emitted during volcanic
84 eruptions and the reduced albedo of glacier surfaces by the deposition of volcanic ash have
85 notably contributed to rapid glacier recession in these areas (Granados et al., 2015; Huggel et
86 al., 2007; Rabatel et al., 2013; Vuille et al., 2017).

87 Current glacier recession in the Andes involves the loss of natural scientific laboratories (Francou
88 et al., 2003) and of landscape and cultural emblems of mountainous areas (IDEAM, 2012; Rabatel
89 et al., 2017). But in more practical terms, the vanishing of glaciers has a major impact on
90 livelihoods of communities living downstream, including potential reduction of freshwater storage
91 and changes in the seasonal patterns of water supply by downstream rivers (Kaser et al., 2010).
92 Glaciers constitute natural water reservoirs in the form of ice accumulated during cold and wet
93 seasons, and they provide water when ice melts during above-freezing temperature seasons.
94 The hydrological importance of glaciers for downstream areas depends on the availability of other
95 sources of runoff, including snow melt and rainfall. Therefore, water supply by glaciers becomes
96 critical for arid or semi-arid regions downstream of the glacierized areas, buffering the lack of
97 sustained precipitation or water provided by seasonal melt of snow cover (Rabatel et al., 2013;
98 Vuille et al., 2008). Such is the case for the western slopes of the tropical Andes: in countries like
99 Peru or Bolivia, with a high variability in precipitation and a sustained dry season, the contribution
100 of glacier melt is crucial for socioeconomic activities and for water supply, especially since it is
101 one of the main sources of water for the highly populated capital cities such as La Paz (Kaser et
102 al., 2010; López-Moreno et al., 2014; Soruco et al., 2015; Vuille et al., 2017). In more
103 humid/temperate regions (i.e. the Alps or western North America) the melt of seasonal snow
104 cover provides the majority of water during the melt season (Beniston, 2012; Stewart et al., 2004)

105 and glacier melt is a secondary contributor. However, even in this region, water availability can
106 be subject to climate variability, and the occurrence of dry and warm periods that comprise thin
107 and brief snow cover may involve glacier melt as the main source of water during such events
108 (Kaser et al., 2010). In the inner tropics, glaciers may not constitute the main source of water for
109 downstream populations, as the seasonal shift of the Intertropical Convergence Zone (Poveda et
110 al., 2006) assures two humid seasons every year; however, the loss of water from glacier melt
111 can affect the eco-hydrological functioning of the wetland ecosystems called “*páramos*”, which
112 are positioned in the altitudinal tier located below that of the periglacial ecosystem (Rabatel et al.,
113 2017). Agriculture and livestock in Colombian mountain communities are partly dependent on
114 water from these important water reservoirs that provide water flow to downstream rivers, even
115 during periods of less precipitation.
116

117 **1.2. Hypothesis and objectives**

118 The present work is focused on the hydrological dynamics of a Colombian glacier near extinction
119 due to prolonged deglaciation. Hock et al. (2005) presented a summary of the effects of glaciers
120 on streamflow compared to non-glacierized areas. The main characteristics of streamflow can be
121 summarized as follows (Hock et al., 2005):

- 122 - Specific runoff dependence on variability of glacier mass balance. In years of mass
123 balance loss, total streamflow will increase as water is released from glacier storage. The
124 opposite will happen in years of positive mass balance.
- 125 - Seasonal runoff variation dependent on ablation and accumulation periods at latitudes
126 with markedly variable temperature and/or precipitation seasonal patterns. In the case of
127 temperature, this does not apply to glaciers in the inner tropics
- 128 - Large diurnal fluctuation in the absence of precipitation, as a result of the daily cycle of
129 temperature and derived glacier melt.
- 130 - Moderation of year-to-year variability. Moderate percentages (10 to 40%) of ice cover
131 fraction within the basin reduces variability to a minimum, but it becomes greater at both
132 higher and lower glacierization levels.
- 133 - Large glacierization involves a high correlation between runoff and temperature, whereas
134 low levels of glacier cover increase runoff correlation with precipitation.

135 However, under warming conditions that lead to glacier retreat, the hydrological contribution of
136 the glacier may notably change from the aforementioned characteristics. The retreat of a glacier
137 is a consequence of prolonged periods of negative mass balance, the result of a disequilibrium
138 in the accumulation/ablation ratio that involves an upward shift of the equilibrium line (the
139 elevation at which accumulation and ablation volumes are equal) and an increase of the ablation
140 area with respect to the accumulation area (Chevallier et al., 2011). As a result, the glacierized
141 area is increasingly smaller compared to the non-glacierized area within the catchment in which
142 the glacier is settled. Under such conditions of sustained negative mass balance, the hydrological
143 response of the glacier will be a matter of time-scales (Chevallier et al., 2011; Hock et al.,
144 2005). The total runoff production of the retreating glacier comprises a tradeoff between two
145 processes: on one side, an acceleration of glacier melt that will increase the volume of glacier
146 outflows, independent of the volume precipitated as snowfall or rainfall; on the other side, water
147 discharges from the catchment decrease because the water reservoir that represents the glacier
148 is progressively emptying (Huss and Hock, 2018). Thus, the contribution of glacier melt to total
149 water discharge will initially increase, as the first process will dominate over the other; however,
150 after reaching a discharge peak, the second process dominates, leading to a decrease in water
151 discharge until the glacier vanishes. In terms of runoff variability, there is also a different signal
152 between initial and final stages of glacier retreat: on a daily basis, the typical diurnal cycle of
153 glacier melt will exacerbate at the initial stages (larger difference between peak and base runoff)
154 and will moderate at the final stages. However, in terms of year-to-year variability, there can be
155 a reduction or increase at the initial stages, depending on the original glacierized area. And for
156 the long term, increasing variability should be expected, as the water discharge will correlate with
157 precipitation instead of temperature because the percentage of runoff from glacier melt decreases
158 with decreasing glacierization (Hock et al., 2005).

159 It is expected that changes will be observed in the hydrological dynamics of vanishing glaciers,
160 independently of climate drivers. Such hydrological changes may serve as indicators of glacier
161 shrinkage, complementing others such as mass balance or areal observations. The objective of
162 this work is to provide a comprehensive analysis of the hydrological dynamics of a glacierized
163 basin, with the glacier in its last stages prior to extinction. Considering the abovementioned
164 characteristics of the hydrology of retreating glaciers, the specific aim is to explore changes on
165 time of streamflow dynamics, focusing on the daily cycle, and to discern whether such changes
166 are driven by climate or are a result of the diminishing glacierized area within the basin.

167 The case study is a small glacier (see description in Section 2) in the Central Colombian Andes
168 and the catchment that drains the water at the snout of the glacier. It is one of the very few
169 monitored glaciers in the tropical Andes (Mölg et al., 2017; Rabatel et al., 2017) and represents
170 an ideal case, where the hydrological signal of the glacier can be studied in isolation from any
171 environmental factors that may occur in the downstream areas. For this reason, the approach
172 used (see Section 3.3) can be applied to similar environments, and the obtained results can be
173 representative of expected hydrological dynamics in other glacierized areas in the Andes, with
174 glaciers close to extinction.

175

176 **2. Study site**

177 Our study focuses on the Conejeras glacier, a very small ice mass (14 hectares in 2017) that
178 forms part of a larger glacier system called Nevado de Santa Isabel (1.8 km²), one of the six
179 glaciers that still persist in Colombia. It is located in the Cordillera Central (the central range of
180 the three branches of the Andean chain in Colombia) and, together with the glaciers of Nevado
181 del Ruiz and Tolima, comprises the protected area called Parque Nacional Natural de los
182 Nevados (Fig. 1). The summit of the Santa Isabel glacier reaches 5100 m, being the lowest glacier
183 in Colombia. As a result, it is as well the most sensitive to atmospheric warming and why it has
184 been monitored since 2006, part of the world network of glacier monitoring (IDEAM, 2012). The
185 Santa Isabel glacier has been retreating since the 19th century, with an intensification of
186 deglaciation since the middle of the 20th century. As a result, the glacier is now a set of separated
187 ice fragments instead of a continuous ice mass, as it was a decade ago (IDEAM, 2012). One of
188 the fragments, located at the north-east sector of the glacier, is the Conejeras glacier, which is
189 the object of this study, whose elevation ranges between 4700 and 4895 m. In 2006, at the glacier
190 terminus, hydro-meteorological stations were installed in order to measure glacier contribution to
191 runoff, as well as air temperature and precipitation.

192 The Conejeras water stream is a tributary of one of the 'quebradas' (Spanish for small mountain
193 rivers in South American countries) flowing into the river Rio Claro. Thus, the Conejeras glacier
194 corresponds to the uppermost headwaters of the Rio Claro basin (Fig. 1). The Rio Claro basin
195 comprises an elevation range of 2700 to 4895 m and, from highest to lowest, presents a
196 succession of typical Andean ecosystems: glacial (4700 to 4894), periglacial (4300 – 4700 m),
197 *páramo* wetland ecosystem (3600 to 4300 m) and high elevation tropical forest *bosque altoandino*
198 (2700 to 3600 m). Mean annual temperature at the glacier base is $1.3 \pm 0.7^{\circ}\text{C}$, with very little
199 seasonal variation, and precipitation sums reach 1025 ± 50 mm annually, with two contrasted
200 seasons (see Figure 2) resulting from the seasonal migration of the Intertropical Convergence
201 Zone (ITCZ, Poveda et al., 2006). During the dry seasons (December to January and June to
202 August), mean precipitation barely reaches 75 mm per month, whereas during the wet seasons
203 (March to May and September to October), values exceed 150 mm per month.

204

205

206

207

208 **3. Data and Methods**

209

210 **3.1. Hydrological and meteorological data**

211 Meteorological and hydrological data used in the present work have been collected by the Institute
212 for Hydrological, Meteorological and Environmental Studies of Colombia (IDEAM, *Instituto de*
213 *Hidrología, Meteorología y Estudios Ambientales*), thanks to the automatic meteorological and
214 gauge stations network at the Río Claro basin (Figure 1).

215 The experimental site of the Río Claro basin has been monitored since 2009, with a network of
216 meteorological and hydrological stations located at different tributaries of the Río Claro River,
217 covering an altitudinal gradient of 2700 – 4900 m.asl. As this research is focused on the upper
218 catchment in which the glacier is located for the present study, we used data from just the stations
219 located at the Conejeras glacier snout (Figure 1, bottom map). This includes one stream gauge
220 (with associated rating curve) measuring 15-minute resolution water discharge ($\text{m}^3 \text{s}^{-1}$); one
221 temperature station measuring hourly temperature ($^{\circ}\text{C}$) (both stations located at 4662 m.asl); and
222 one rain-gauge measuring 10-minute precipitation (mm, the station located at 4413 m. asl). Even
223 though these data have been available since 2009, the sensors and loggers experienced
224 technical problems; thus, numerous inhomogeneities, out-of-range values and empty records
225 were present in the data series. From 2013, the technical problems were solved and the data is
226 suitable for analysis. The period covered for analysis ranges from June 2013 to December 2017,
227 a total of 56 months, and data was aggregated hourly, daily and monthly to perform statistical
228 analyses. However, in order to obtain a wider perspective and to take advantage of the effort
229 made by the IDEAM glaciologist, who conscientiously took mass balance measurements every
230 month since 2006, also shown are trends and variability in climate from a nearby meteorological
231 station of the Colombian national network (Brisas), that contains data since 1982 and glacier
232 mass evolution for the longest time period available. The Multivariate ENSO Index, used for
233 characterizing influence of the ENSO phenomenon on glacier evolution has been downloaded
234 from NOAA <https://www.esrl.noaa.gov/psd/enso/mei/table.html> (December 2017).

235

236 **3.2. Glacier evolution data**

237 The evolution of the Conejeras glacier (Fig. 3) has been monitored by the Department of
238 Ecosystems of IDEAM. Since March 2006, a network of 14 stakes was installed on the Conejeras
239 glacier to measure ablation and accumulation area. The 6–12 m long stakes are PVC pipes of 2
240 m in length. These 14 stakes are vertically inserted into the glacier at a depth not less than 5
241 meters and they are roughly organized in six cross profiles at approximately 4670, 4700, 4750,
242 4780, 4830 and 4885 m. asl. Accumulation and ablation measurements are performed monthly.
243 Typical measurements of the field surveys include stake readings (monthly), density
244 measurement in snow and firn pits (once per year) and re-drilling of stakes (if required) to the
245 former position. The entire methodology can be found in (Mölg et al., 2017; Rabatel et al., 2017).
246 The mass balance data is calculated using the classical glaciological method that represents the
247 water equivalent that a glacier gains or loses in a given time. This data is used to generate yearly
248 mappings of mass balance and calculate the equilibrium line altitude (ELA), which is the altitude
249 point where mass balance is equal to zero equivalent meters of water and separates the ablation
250 and accumulation area in the glacier (Francou and Pouyaud, 2004).

251

252 Changes in glacier surface during the study period were computed by means of satellite imagery
253 (Landsat and Sentinel constellations) for the years 2006, 2010, 2013 and 2017. Cloud-free cover
254 Landsat TM images were selected for 2006 and 2010 years, and Landsat OLI and Sentinel
255 images for 2013 and 2017 respectively. TOA (Top Of Atmosphere) Reflectance was obtained
256 using specific radiometric calibration coefficients for each image and sensor (Chander et al.,
257 2009; Padró et al., 2017). BOA (Bottom of the Atmosphere) Reflectance was based on the Dark
258 Object Substraction (DOS) approach (Chavez, 1988). The Normalized Difference Snow Index
259 (NDSI) was used to discriminate snow and ice-covered areas from snow-free areas. The NDSI is
260 expressed as the relationship between reflectance in the visible region and reflectance in the
261 medium-infrared region (the specific bands vary among different sensors; e.g. TM bands 2 and
262 5). Pixels in the different images were classified as snow- or ice-covered areas when the NDSI
263 was greater than 0.4 (Dozier, 1989).

264

265

266 **3.3. Statistical Analyses**

267 A number of indices were extracted from the streamflow, temperature and precipitation hourly
268 series in order to assess changes in time in the hydrological output of the glacier and their relation
269 to climate (Table 1). These daily indices were subject to statistical analyses, including correlation
270 tests, monthly aggregation and assessment of changes over time.

271 Since one of the main objectives of the paper is to characterize daily dynamics of streamflow and
272 changes in time, a principal component analysis (PCA) was conducted in order to extract the
273 main patterns of daily streamflow cycles. The data matrix for the PCA was then composed by
274 streamflow hourly values in 1614 columns as variables (number of days) and 24 rows as cases
275 (hours in a day). As the PCA does not allow the number of variables to exceed the number of
276 cases, PCAs were performed on 25 bootstrapped random samples of days ($n=23$, with
277 replacement); Results showed that three principal components were stable throughout the
278 samples (see Table 3 in Results sections). After the main PCs were extracted, calculation of
279 correlation between each day of the time series and the selected PCs was determined. The PC
280 that best correlated with the correspondent day was assigned to every day, obtaining a time-
281 series of the three PCs. This allowed assessment of changes in time of the main patterns of daily
282 streamflow cycles observed.

283

284 **4. Results**

285 **4.1. Climatology and glacier evolution**

286 The long-term climatic evolution of the study area is depicted in Figure 2. The temperature and
287 precipitation series (Fig. 2 a, c and d) correspond to the Brisas meteorological station, which is
288 located 25 km from the glacier, at 2721 m elevation. It therefore does not accurately represent
289 the climate conditions at the glacier. It is, however, the closest meteorological station with
290 available meteorological data to study long-term climate. The temperature record measured at
291 the glacier snout (blue line) is included. It can be observed that despite the different range of
292 values (temperatures at the glacier are 3.2 °C lower than at Brisas), there is a match in variability
293 for the common period.

294 Long-term evolution of temperature does not show any significant trend or pattern from 1982 to
295 2015; however, a spectral analysis shows that the frequency with higher spectral density
296 corresponds with a seasonality of 48 months, indicating a recurrent cycle every four years. By
297 comparing Fig. 2a with Fig. 2b, there is a close match between temperature and evolution of the
298 Multivariate ENSO Index ($R = 0.49$), which also shows a high value of power spectra in the 48-
299 month frequency cycle. Notwithstanding other factors whose analysis is far beyond the scope of
300 this paper, it is evident that the evolution of temperature in the study area is highly driven by the
301 ENSO phenomenon. Regarding precipitation (Fig. 2c), no long-term trend is observed, and the
302 most evident pattern is the bi-modal seasonal regime which is confirmed by the frequency
303 analysis showing the highest power spectra in the 6-month cycle.

304 The evolution of the glacier since 2006 is shown in Figure 3. Almost every month since
305 measurements began in 2006, the glacier has lost mass (113 months), and very few months (20)
306 recorded a positive mass balance. The global balance in this period is a loss of 34.4 meters of
307 water equivalent. For the sake of visual comparison, we have included the time series of MEI,
308 and a close correspondence between the variables is observed (Figure 3.a). During the warm
309 phases of ENSO (Niño events, values of MEI above 0.5), the glacier loses up to 600 mm w.e. per
310 month, as in the Niño event of 2009-2010, when the glacier lost a total of 7000 mm w.e. One
311 could surmise that during La Niña (cold phases of ENSO, MEI values < -0.5) the glacier could
312 recuperate mass. In fact, when MEI values are negative, the glacier experiences much less
313 decrease; however, even during the strongest La Niña events, the balance is negative, with just
314 a few months having a positive balance (e.g. in the 2010-2011 La Niña, the glacier lost 1000 mm
315 w.e.) This occurs because even during La Niña mean temperatures at the glacier are above zero
316 (0.8 ± 0.3 °C). The aforementioned agreement between ENSO and mass balance appears to
317 break from 2012 onwards. There were two events of large mass balance loss around 2013-2014
318 that do not match with El Niño events. A local factor that can affect the glacier's mass balance
319 independent of climatology is reduced albedo of the surface caused by the quantity of deposited
320 ash that comes from the nearby Santa Isabel volcano. This variable has not been considered in

321 the present study but there are two pictures of the glacier for visual evidence (Figure 3.d). This
322 fact, together with prevalence of above-zero degrees at the elevation in which the glacier is
323 located (see Figure 2, top plot) has induced the large glacier recession observed between 2006
324 and 2017 (Figure 3.c). During this period, there has been a 37% reduction, from 22.45 ha in 2006
325 to 12 ha in 2017. However, this reduction has been far from linear. As shown in Figure 3.b, mass
326 balance losses during the first years of the monitoring period were, in general, less pronounced
327 than in the latest years. In 2012, the ice mass retreated up the 4700 m elevation curve, and from
328 then on the years with larger mass loss were 2015, 2016 and 2014.

329

330 4.2. Hydrological dynamics

331 The water discharge of the Conejeras glacier is measured at a gauging station located 300 m
332 from the glacier snout (when the station was installed in 2009, it was only 10 meters away from
333 the glacier snout). The water volume measured at this station is a combination of water from
334 glacier melt and water from precipitation into the watershed area, although the former exerts a
335 larger control in water discharge variability. Table 2 shows the correlation between hydrological
336 and temperature indices for samples of days with precipitation, independent of the amount of
337 fallen precipitation (left), and for samples of days without precipitation (right). On days without
338 precipitation, most hydrological indices show significant correlation with temperature, except for
339 the baseflow and hQ_{max} . The highest correlation values are found between Q_{max} , Q_{range} ,
340 Q_{slope} and $totalQ$, with T_{max} and T_{mean} (correlation values in the range of 0.5 – 0.65), indicating
341 that the higher the temperatures, the more prominent the melting pulse of runoff. T_{min} shows
342 smaller and less significant correlation values. The $hpulse$ also shows high correlation with
343 temperature, but in this case in a negative fashion, indicating a later occurrence of the daily
344 melting pulse when minimum temperatures and maximum temperatures are lower. On days with
345 precipitation, correlation values are generally smaller but, in some cases, they are still significant
346 as for Q_{max} , Q_{range} and Q_{slope} .

347 A Principal Component Analysis (PCA) performed on hourly streamflow data (in a recursive
348 fashion, see Section 3.3 for explanation of the method) allowed procurement of the main patterns
349 of daily flow, as well as changes in time during the study period. Three principal components were
350 obtained, whose values of explained variance were stable throughout the 25 bootstrapped
351 samples (Table 3). The first PC explained an average of $48 \pm 6\%$ of the variance throughout the
352 25 samples, and the second PC an average of $35 \pm 5.7\%$. Together they account for 83% of
353 variance and they both showed a neat pattern of daily streamflows (Fig. 4a). The main difference
354 between PC1 and PC2 is the time of the day when peak flows are reached and, hence, the time
355 range when most daily flows occur. Thus, PC1 corresponds to days with an earlier melt pulse
356 (towards 10h) and earlier peak flows (towards 14h), compared to PC2, with days of melt pulse at
357 13h and peak flows at 18h. The remaining PC explains a residual percentage of the variance and,
358 unlike PC1 and PC2, does not show a stable streamflow pattern across the samples. However, it
359 was decided to keep it, as it can help explain some peculiarities in the results. In Figure 4b the
360 evolution of the frequency (days per month) of days corresponding to each PC is shown. Although
361 there is some degree of variability, the frequency of days with PC1 streamflow pattern increases
362 over time and dominates over the frequency of PC2 and PC3 days. This is especially significant
363 between 2015 and 2016, coinciding with an El Niño event. However, by mid-2016 the frequency
364 of PC1 days drops considerably and the frequency of PC2 days increases in the same ratio. Thus,
365 from mid-2016 to the end of the study period, they both maintain similar levels of frequency.

366 In order to understand the underlying factors of each PC, the frequency distribution of the climatic
367 and hydrological indices for the days corresponding to each PC was computed, in the form of
368 boxplots (Figure 5). From a hydrological point of view, PC1 better corresponds to days with higher
369 total runoff and maximum runoff, and with a more pronounced slope in both the rising and
370 decreasing limbs of the peak flow volume than PC2 and PC3. The variability (expressed by the
371 amplitude of boxes in the boxplots) of such hydrological indicators is, as well, higher amongst
372 days of PC1, compared to days of PC2 and PC3. Base runoff is higher in PC1 but not significantly.
373 The contrasted weight of climate may explain such hydrological differences between PCs: days
374 of PC1 present significantly higher mean temperature (median = 1.7°C) and maximum
375 temperature (median = 3.8°C) than days of PC2 (0.9°C and 2.4°C respectively) and PC3 (0.5°C

376 and 1.6°C respectively). In contrast, precipitation is notably higher (and shows greater variability)
377 in days grouped within PC3 (median = 1.9 mm day⁻¹) and PC2 (2.2 mm day⁻¹) compared to days
378 of PC1 (0.3 mm day⁻¹). To summarize, PC1 corresponds to a daily regimen of pure glacier melting,
379 whereas PC2 and PC3 correspond to days with a lower glacier melting pulse with more (PC3) or
380 less (PC2) influence of precipitation.

381

382

383

384 In Figure 4, a notable change occurs in the frequency of the two main patterns of hourly
385 streamflow, PC1 and PC2, by mid-2016. Further details regarding changes in the hydrological
386 yield of the glacier are shown in Figure 6, which presents the evolution of the main hydrological
387 indices computed, along with temperature, precipitation and glacier mass balance during the
388 study period and averaged monthly. Total and maximum daily streamflow (*totalQ* and *Qmax*)
389 depict an increase up to mid-2016, where they begin to decrease. During the last 18 months, they
390 remain at low levels compared to previous months. This turning point seems to coincide in time
391 with the 2015-16 El Niño event, with higher-than-average temperatures and low levels of
392 precipitation that led to an increasing mass balance loss and, therefore, increased flows. It is
393 remarkable that streamflow increases and decreases in direct proportion to mass balance
394 change, indicating the strong dependence of runoff to glacier melt. Similar evolution is observed
395 in the difference between base flows and maximum flows (*Qrange*), as well as the slope of the
396 rising limb of diurnal flows (*Qslope*) which are indicators of diurnal variability: they increase up to
397 2016 and decrease afterwards, which coincides with the change in the frequency of daily
398 streamflow patterns in Fig. 5. The mean hour of the day at which maximum flows are reached
399 (*hQmax*) shows a steady evolution until mid-2016, when it begins to rise. This seems surprising
400 when comparing it to the evolution of *hTmax* (i.e. the hour of the day when maximum temperature
401 is reached), which does not show any particular temporal pattern. Regarding the monthly
402 variability of flows (third panel on the right, Fig. 7) the same turning point is observed, with a clear
403 decrease in the coefficient of variation until 2016 and an increase afterwards. It is clear that a
404 hydrological change has occurred at the outlet of the glacier, but the two most plausible drivers
405 of change (temperature and precipitation, bottom plots Fig. 7) do not seem to be responsible for
406 it. They both are affected by the El Niño event, when temperatures increased and precipitation
407 decreased; however, they do not show an increasing-decreasing temporal pattern before and
408 after such an event. This leads to the hypothesis that the hydrological change observed at these
409 last stages of the glacier's life is independent of climate.

410

411

412 **4.3. Changes in the runoff-climate relationship**

413 In this section, the runoff is isolated from temperature and precipitation in order to determine if
414 observed hydrological dynamics are driven by climate or are related to shrinkage of the glacier.
415 Figure 7 shows the mean monthly runoff for days with temperatures lower and higher than 2°C,
416 i.e. water discharge series independent of temperature. Precipitation has also been added to the
417 plot. It was noted that water discharge for days warmer than 2°C is significantly higher than water
418 discharge on days cooler than 2°C. The characteristic evolution of runoff, with increasing amounts
419 during most of the study period up to mid-2016 and decreasing runoff from that point onwards,
420 was also observed. The same evolution occurs for both days below and days above 2°C, and it
421 occurs for very similar amounts of precipitation. This indicates that flows from the melting glacier
422 are becoming less dependent on temperature, or climate in general, and more dependent on the
423 size of the glacier. The boxplots of Figure 8 (bottom) confirm this observation by showing water
424 volumes significantly higher before than after the breaking point, but also because the differences
425 between water discharge at < 2°C and water discharge at > 2°C are also smaller (and not
426 significant) after the breaking point, indicating the decreasing importance of temperature in the
427 process of runoff production in the shrinking glacier.

428 Finally, Figure 8 shows correlations between temperature/precipitation and monthly flows for
429 different time periods. In Figure 8a, two years are compared that can be considered analogues in
430 terms of total flow (similar amounts of monthly flow, see Figure 6), but one year (2013-14) belongs
431 to the period of increasing flows, before the 2016 breakpoint, and the other year (2017) belongs
432 to the period of decreasing flows after the breakpoint. Correlation between temperature and flow
433 is much higher ($R = 0.65$) for 2013-14 than for 2017 ($R = 0.35$), which would corroborate the
434 previous observation. However, precipitation also shows higher correlation with flow for 2013-14
435 ($R = 0.67$) than for 2017 ($R = 0.42$), which would contradict the hypothesis. One year, however,
436 may not be representative of general trends, and so the same analysis is repeated, not for
437 individual years but for the whole periods pre- and post-2016 breakpoint (Fig. 8b). The pattern
438 seems more clear and corroborates the aforementioned hypothesis: correlation between
439 temperature and flow is significant for the pre-2016 period ($R = 0.55$) but is non-existent for the
440 post-2016 period ($R = -0.1$). Correlation between precipitation and flow is insignificant ($R = -0.23$)
441 for the pre-2016 period, and it is positive and significant for the post-2016 period ($R = 0.32$). These
442 previous observations lead to reasoning that during the years of hydrological monitoring (2013-
443 2017), the observed hydrological dynamic, with a marked breakpoint in 2016, is a result of the
444 vanishing glacier process and not a response to climate variability.

445

446 5. Discussion and conclusions

447 The present paper shows a comprehensive analysis of the dynamics of an Andean glacier that is
448 close to extinction, with special focus on its hydrological yield. This research has benefited from
449 a hydro-climatic monitoring network located in the surroundings of the glacier terminus that has
450 been fully operative since 2013 and from monthly and annual estimations of mass balance and
451 glacier extent respectively, derived from ice depth measurements and topographical surveys
452 since 2006. Everything has been managed by the Institute of Hydrology Meteorology and
453 Environmental Studies (IDEAM) of Colombia. The *Conejeras* glacier is currently an isolated small
454 glacier that used to be part of a larger ice body called *Nevado de Santa Isabel*. Since
455 measurements have been available, the glacier has constantly lost mass and, consequently, a
456 reduction in its area is evident. The extinction of Colombian glaciers has been documented since
457 1850, with an average loss of 90% of their area, considering current values (IDEAM, 2012). This
458 reduction, of about 3% per year, has been much larger during the last three decades (57%)
459 compared to previous decades (23%), which is directly related to the general increase in
460 temperatures in the region and to re-activation of volcanic activity (IDEAM, 2012; Rabatel et al.,
461 2017). Since direct measurements began in 2006, the studied glacier has constantly lost area;
462 however, until 2014, the area loss was gradual and restricted to the glacier front; from 2014, the
463 sharp retreat also involved higher parts of the glacier. The main reason for this strong shrinkage
464 is the existence of above-zero temperatures during most of the year and less precipitation fallen
465 as snow. This involves a constant migration of the equilibrium line to higher positions, and
466 decreasing albedo of the ice surface that involves greater energy absorption, the latter
467 accelerated by intense activity of Nevado de el Ruiz in the last years. In terms of mass balance,
468 very few months exhibit a gain of ice during the studied period, and these tend to coincide with la
469 Niña events (negative MEI episodes). These episodes cannot compensate for the great losses
470 that occurred during the majority of months, which are especially large during El Niño events
471 (positive MEI episodes), when above-normal temperatures are recorded. The ENSO
472 phenomenon exerts great influence on the evolution of the glacier, similar to that reported for
473 most inner tropical glaciers (Francou et al., 2004; Rabatel et al., 2013; Vuille et al., 2008);
474 however, some episodes of great mass balance loss, such as that of 2014, cannot be explained
475 by the ENSO. Observations of glacier surface during field surveys showed that, during some
476 periods of mass loss, surface ice retreat left ancient layers of volcanic ash exposed. The reduced
477 energy reflectance caused by such ash layers might have triggered positive feedback that led to
478 increasing melting and large ice retreat.

479 Glacier retreat is a worldwide phenomenon, currently linked to global warming (IPCC, 2013).
480 Amongst the environmental issues related to glacier retreat, the issue concerning water resources
481 has produced a vast amount of research. This is because glaciers constitute water reservoirs in
482 the form of accumulated ice over thousands of years, and they provide water supply to
483 downstream areas for the benefit of life, ecosystems and human societies. The rapid decrease in

484 glacier extent during the last decades involves a change in water availability in glacier-dominated
485 regions, and, thus, changes in water policies and water management are advisable (Huss, 2011;
486 Kundzewicz et al., 2008). In the short term, glacier retreat involves increasing runoff in
487 downstream areas but, after reaching a peak, runoff will eventually decrease until the contribution
488 of the glacier melt is zero, when the glacier completely disappears. From a global perspective,
489 such a tipping point is referred to as *peak water* and has given rise to concern from the scientific
490 community (Gleick and Palaniappan, 2010; Huss and Hock, 2018; Kundzewicz et al., 2008; Mark
491 et al., 2017; Sorg et al., 2014). Research regarding the occurrence of such a runoff peak related
492 to glacier retreat demonstrates that it will not occur concurrently worldwide. In some mountain
493 areas, it has already occurred, i.e. the Peruvian Andes (Baraer et al., 2012), the Western U.S
494 mountains (Frans et al., 2016) or Central Asia (Sorg et al., 2012). At the majority of studied glacier
495 basins, it is expected to occur in the course of the present century (Immerzeel et al., 2013; Ragettili
496 et al., 2016; Sorg et al., 2014; Soruco et al., 2015). In recent global-scale research, Huss and
497 Hock (2018) state that in nearly half of the 56 large-scale glacierized drainage basins studied, the
498 peak water has already occurred. In the other half, it will occur in the next decades, depending
499 on extension of the ice cover fraction.

500 It was not the aim of this study to allocate such a tipping point in our studied glacier; however,
501 observations on the characteristics of streamflow along the studied period suggest that it may
502 have occurred during our study period. Our observations corroborate glacier melt being the main
503 contributor to runoff in the catchment. However, even when correlations between runoff and
504 temperature are mostly significant, the values are not as high as could be expected for a
505 glacierized catchment. This is due to decreasing dependence of runoff on temperature, and
506 therefore to glacier melt, as at a specific point during the study period. We observed a changing
507 dynamic in most hydrological indicators, with a turning point in mid-2016, whereas climate
508 variables, i.e. temperature and precipitation, do not show such evident variation (besides the
509 exceptional conditions during an El Niño event). Both the PCA analysis and the monthly
510 aggregation of hydrological indices point to a less glacier-induced hydrological yield once the
511 runoff peak of 2016 was reached. According to literature (see Section 1.2.) this change from
512 increasing to decreasing runoff, and to lesser importance of glacier contributions to total water
513 discharge, must be expected in glacierized catchments with glaciers close to extinction. The short
514 length of our hydrological series (five years) does not allow long-term analysis to determine water
515 discharge in years of less glacier loss (i.e. from 2006 to 2012, see Fig. 3), which could verify or
516 refute such a hypothesis. However, when we isolated total runoff from climate variables before
517 and after the 2016 breakpoint (Figures 8 and 9), we observed that the increase and later decrease
518 of flows was mostly independent of temperature and precipitation, which would involve a glacier-
519 driven hydrological change. Summarizing, streamflow measured at the glacier's snout showed
520 the following characteristics: increasing trend in flow volume until mid-2016 and decreasing trend
521 thereafter; increasing diurnal variability (given by the range between high flows and low flows and
522 by the slope of the rising flow limb) up to mid-2016 and decreasing thereafter; decreasing and
523 increasing monthly variability (given by the coefficient of variation of flows within a given month)
524 before and after such date; and high dependence of flow on temperatures before 2016 and low
525 or null dependence after 2016, with increasing dependence on precipitation. As well, this is
526 supported by an evident change in the type of hydrograph, from a prevalence of days with melt-
527 driven hydrographs (low baseflows, sharp melting pulse and great difference between high flows
528 and low flows) before 2016, to an increase in the occurrence of days with less influence of melt
529 and more influence by precipitation. All these characteristics support the idea of a hydrological
530 change driven by the glacier recession in the catchment, as summarized by Hock et al. (2005,
531 see Section 1.2). This observation cannot be taken conclusively, because the time period of
532 hydrological observation is not long enough to deduce long-term trends and to explore
533 hydrological dynamics before the great decline in glacier extent in 2014. However, given the
534 current reduced size of the glacier (14 hectares, which represents 35% of the catchment that
535 drains into the gauge station), it is likely that water discharge will continue to decrease in the
536 upcoming years, until glacier contribution ends and runoff depends only on the precipitation that
537 falls within the catchment. Like this glacier, other small glaciers in Colombia are expected to
538 disappear in the coming decades (Rabatel et al., 2017); thus, a similar hydrological response can
539 be expected.

540 Unlike glaciers in the western semi-arid slopes of the Andes (i.e. Peru, Bolivia), Colombian
541 glaciers do not constitute the main source of freshwater for downstream populations (IDEAM,
542 2012). The succession of humid periods provides enough water in mountain areas, most of which
543 is stored in the deep soils of *Páramos*. These wetland ecosystems are mainly fed by rainfall (the
544 contribution of glacier melt is mostly unknown, IDEAM, 2012) and act as water buffers, ensuring
545 water availability during not-so-humid periods. Therefore, the role of glaciers in Colombia
546 regarding water resources, including the studied ice body, is more marginal, and the occurrence
547 of the *peak water* from glacier melt is not a current concern, as it is in Peru or Bolivia (Francou et
548 al., 2014). Yet this does not diminish the relevance of the results of this work because they may
549 be taken as an example of what can happen to the hydrology of glacierized basins in the tropics
550 whose glaciers are in the process of disappearing. The studied glacier has a very small size
551 compared to other ice bodies in the region. This makes it respond rapidly to variations in climate,
552 as well as involving a rapid hydrological response of the catchment to the loss of ice, as was
553 observed in this work. The increasing/decreasing flow dynamic observed as the glacier retreated
554 occurred in roughly five years, and this is most likely related to the reduced size of the studied
555 glacier. Most studies on the hydrological response to glacier retreat consider large river basins
556 with large glacier coverage, usually by modeling approaches (i.e. Huss and Hock, 2018;
557 Immerzeel et al., 2013; Ragetti et al., 2016; Sorg et al., 2014, 2012; Stahl et al., 2008), and the
558 response times reported on either increasing flow at the initial stages or decreasing flow at the
559 final stages are always on the scale of decades.

560 The added value of studying the hydrology related to this small-sized and near-extinct glacier is
561 that the changes observed in the hydrology of the catchment could be directly attributed to the
562 dynamics of the glacier and the climate that occurs at the same time-scale; contrary to catchments
563 containing large glaciers that respond with a larger temporal inertia to environmental changes.
564 Hydrological analyses were restricted to the upper catchment because the streamflows measured
565 at the snout of the glacier are not influenced by the signals of other environmental processes that
566 may occur downstream (e.g., forest clearing or increasing grazing). The methodological
567 approach, including the PCA and the hydrological indices computed over sub-daily resolution
568 data demonstrated itself as viable for detecting changes on the diurnal cycle of the glacier and
569 can be applied to other small glaciers of the tropical Andes that respond rapidly (at sub-annual
570 scales) to environmental forcing. The necessity for in situ observations on a fine scale in order to
571 improve accuracy on future estimations of water availability related to glacier retreat is
572 emphasized.

573

574 **Acknowledgments**

575 This work has been possible thanks to the monitoring network installed by the Department of
576 Ecosystems of the Colombian Institute for Hydrology, Meteorology and Environmental Studies
577 (*Instituto de Hidrología, Meteorología y Estudios Ambientales*, IDEAM) and to the monthly field
578 surveys on the Conejeras glacier and Río Claro River basin, done by employed staff. Our sincere
579 gratitude to them, with special thanks to Yina Paola Nocua. The following projects gave economic
580 support to this paper: “*Estudio hidrológico de la montaña altoandina (Colombia) y su respuesta a*
581 *procesos de cambio global*” financed by Banco Santander, through the program of exchange
582 scholarships for young researchers in Ibero-America “*Becas Iberoamérica Jóvenes Profesores e*
583 *Investigadores* (2015); and CGL2017- 82216-R (HIDROIBERNIEVE) funded by the Spanish
584 Ministry of Economy and Competitiveness. We are thankful to the anonymous referees for their
585 valuable comments and suggestions that helped improve the final version of this manuscript.

586

587

588

589

590 **6. References**

591 Baraer, M., Mark, B. G., McKenzie, J. M., Condom, T., Bury, J., Huh, K.-I., Portocarrero, C.,
592 Gómez, J. and Rathay, S.: Glacier recession and water resources in Peru’s Cordillera Blanca, J.

593 Glaciol., 58(207), 134–150, doi:10.3189/2012JoG11J186, 2012.

594 Beniston, M.: Impacts of climatic change on water and associated economic activities in the
595 Swiss Alps, *J. Hydrol.*, 412–413, 291–296, doi:10.1016/J.JHYDROL.2010.06.046, 2012.

596 Bradley, R. S., Vuille, M., Diaz, H. F. and Vergara, W.: Climate change. Threats to water
597 supplies in the tropical Andes., *Science*, 312(5781), 1755–6, doi:10.1126/science.1128087,
598 2006.

599 Cayan, D. R., Dettinger, M. D., Kammerdiener, S. A., Caprio, J. M., Peterson, D. H., Cayan, D.
600 R., Dettinger, M. D., Kammerdiener, S. A., Caprio, J. M. and Peterson, D. H.: Changes in the
601 Onset of Spring in the Western United States, *Bull. Am. Meteorol. Soc.*, 82(3), 399–415,
602 doi:10.1175/1520-0477(2001)082<0399:CITOOS>2.3.CO;2, 2001.

603 Ceballos, J. L., Euscátegui, C., Ramírez, J., Cañon, M., Huggel, C., Haerberli, W. and Machguth,
604 H.: Fast shrinkage of tropical glaciers in Colombia, *Ann. Glaciol.*, 43, 194–201,
605 doi:10.3189/172756406781812429, 2006.

606 Chander, G., Markham, B. L. and Helder, D. L.: Summary of current radiometric calibration
607 coefficients for Landsat MSS, TM, ETM+, and EO-1 ALI sensors, *Remote Sens. Environ.*,
608 113(5), 893–903, doi:10.1016/J.RSE.2009.01.007, 2009.

609 Chavez, P. S.: An improved dark-object subtraction technique for atmospheric scattering
610 correction of multispectral data, *Remote Sens. Environ.*, 24(3), 459–479, doi:10.1016/0034-
611 4257(88)90019-3, 1988.

612 Chevallier, P., Pouyaud, B., Suarez, W. and Condom, T.: Climate change threats to
613 environment in the tropical Andes: glaciers and water resources, *Reg. Environ. Chang.*, 11(S1),
614 179–187, doi:10.1007/s10113-010-0177-6, 2011.

615 Dozier, J.: Spectral signature of alpine snow cover from the landsat thematic mapper, *Remote
616 Sens. Environ.*, 28, 9–22, doi:10.1016/0034-4257(89)90101-6, 1989.

617 Favier, V., Wagnon, P. and Ribstein, P.: Glaciers of the outer and inner tropics: A different
618 behaviour but a common response to climatic forcing, *Geophys. Res. Lett.*, 31(16), L16403,
619 doi:10.1029/2004GL020654, 2004.

620 Francou, B. and Pouyaud, B.: Metodos de observacion de glaciares en los Andes tropicales :
621 mediciones de terreno y procesamiento de datos : version-1 : 2004, [online] Available from:
622 https://www.researchgate.net/profile/Bernard_Pouyaud/publication/282171220_Metodos_de_observacion_de_glaciares_en_los_Andes_tropicales_mediciones_de_terreno_y_procesamiento_de_datos_version-1_2004/links/561ba9b808ae78721fa0f8ad.pdf (Accessed 12 March 2018),
623
624
625 2004.

626 Francou, B., Vuille, M., Wagnon, P., Mendoza, J. and Sicart, J.: Tropical climate change
627 recorded by a glacier in the central Andes during the last decades of the twentieth century:
628 Chacaltaya, Bolivia, 16°S, *J. Geophys. Res.*, 108(D5), 4154, doi:10.1029/2002JD002959, 2003.

629 Francou, B., Vuille, M., Favier, V. and Cáceres, B.: New evidence for an ENSO impact on low-
630 latitude glaciers: Antizana 15, Andes of Ecuador, 0°28'S, *J. Geophys. Res.*, 109(D18), D18106,
631 doi:10.1029/2003JD004484, 2004.

632 Francou, B., Rabatel, A., Soruco, A., Sicart, J. E., Silvestre, E. E., Ginot, P., Cáceres, B.,
633 Condom, T., Villacís, M., Ceballos, J. L., Lehmann, B., Anthelme, F., Dangles, O., Gomez, J.,
634 Favier, V., Maisincho, L., Jomelli, V., Vuille, M., Wagnon, P., Lejeune, Y., Ramallo, C. and
635 Mendoza, J.: Glaciares de los Andes tropicales: víctimas del cambio climático, Comunidad
636 Andina, PRAA, IRD. [online] Available from:
637 <http://bibliotecavirtual.minam.gob.pe/biam/handle/minam/1686> (Accessed 22 February 2018),
638 2014.

639 Frans, C., Istanbuluoglu, E., Lettenmaier, D. P., Clarke, G., Bohn, T. J. and Stumbaugh, M.:
640 Implications of decadal to century scale glacio-hydrological change for water resources of the
641 Hood River basin, OR, USA, *Hydrol. Process.*, 30(23), 4314–4329, doi:10.1002/hyp.10872,
642 2016.

- 643 Gleick, P. H. and Palaniappan, M.: Peak water limits to freshwater withdrawal and use, *Proc.*
644 *Natl. Acad. Sci.*, 107(25), 11155–11162, doi:10.1073/pnas.1004812107, 2010.
- 645 Granados, H. D., Miranda, P. J., Núñez, G. C., Alzate, B. P., Mothes, P., Roa, H. M., Cáceres
646 Correa, B. E. and Ramos, J. C.: Hazards at Ice-Clad Volcanoes: Phenomena, Processes,
647 and Examples From Mexico, Colombia, Ecuador, and Chile, *Snow Ice-Related Hazards, Risks*
648 *Disasters*, 607–646, doi:10.1016/B978-0-12-394849-6.00017-2, 2015.
- 649 Hock, R., Jansson, P. and Braun, L. N.: Modelling the Response of Mountain Glacier Discharge
650 to Climate Warming, in *Global Change and Mountain Regions (A State of Knowledge*
651 *Overview)*, pp. 243–252, Springer, Dordrecht., 2005.
- 652 Huggel, C., Ceballos, J. L., Pulgarín, B., Ramírez, J. and Thouret, J.-C.: Review and
653 reassessment of hazards owing to volcano–glacier interactions in Colombia, *Ann. Glaciol.*, 45,
654 128–136, doi:10.3189/172756407782282408, 2007.
- 655 Huss, M.: Present and future contribution of glacier storage change to runoff from macroscale
656 drainage basins in Europe, *Water Resour. Res.*, 47(7), doi:10.1029/2010WR010299, 2011.
- 657 Huss, M. and Hock, R.: Global-scale hydrological response to future glacier mass loss, *Nat.*
658 *Clim. Chang.*, 8(2), 135–140, doi:10.1038/s41558-017-0049-x, 2018.
- 659 IDEAM: Glaciares de Colombia, más que montañas con hielo, edited by Comité de
660 Comunicaciones y Publicaciones del IDEAM, Bogotá., 2012.
- 661 Immerzeel, W. W., Pellicciotti, F. and Bierkens, M. F. P.: Rising river flows throughout the
662 twenty-first century in two Himalayan glacierized watersheds, *Nat. Geosci.*, 6(9), 742–745,
663 doi:10.1038/ngeo1896, 2013.
- 664 IPCC: Climate Change 2013: The Physical Science Basis. Contribution of Working Group I to
665 the Fifth Assessment Report of the Intergovernmental Panel on Climate Change, edited by T. F.
666 Stocker, D. Qin, G.-K. Plattner, M. Tignor, S. K. Allen, J. Boschung, A. Nauels, Y. Xia, V. Bex,
667 and P. M. Midgley, Cambridge University Press, Cambridge, United Kingdom and New York,
668 NY, USA., 2013.
- 669 Kaser, G. and Omaston, H.: Tropical glaciers, Cambridge University Press. [online] Available
670 from: [https://books.google.es/books?hl=es&lr=&id=ZEB-](https://books.google.es/books?hl=es&lr=&id=ZEB-I3twN_gC&oi=fnd&pg=PR11&dq=tropical+glaciers&ots=WLwn1fdjig&sig=897EG6q4Pyc113vo9Qb2bnyUo7g#v=onepage&q=tropical+glaciers&f=false)
671 [I3twN_gC&oi=fnd&pg=PR11&dq=tropical+glaciers&ots=WLwn1fdjig&sig=897EG6q4Pyc113vo9](https://books.google.es/books?hl=es&lr=&id=ZEB-I3twN_gC&oi=fnd&pg=PR11&dq=tropical+glaciers&ots=WLwn1fdjig&sig=897EG6q4Pyc113vo9Qb2bnyUo7g#v=onepage&q=tropical+glaciers&f=false)
672 [Qb2bnyUo7g#v=onepage&q=tropical glaciers&f=false](https://books.google.es/books?hl=es&lr=&id=ZEB-I3twN_gC&oi=fnd&pg=PR11&dq=tropical+glaciers&ots=WLwn1fdjig&sig=897EG6q4Pyc113vo9Qb2bnyUo7g#v=onepage&q=tropical+glaciers&f=false) (Accessed 21 November 2017), 2002.
- 673 Kaser, G., Grosshauser, M. and Marzeion, B.: Contribution potential of glaciers to water
674 availability in different climate regimes., *Proc. Natl. Acad. Sci. U. S. A.*, 107(47), 20223–7,
675 doi:10.1073/pnas.1008162107, 2010.
- 676 Klein, A. G., Morris, J. N. and Poole, A. J.: Retreat of Tropical Glaciers in Colombia and
677 Venezuela from 1984 to 2004 as Measured from ASTER and Landsat Images, in 63 rd
678 EASTERN SNOW CONFERENCE, Newark, Delaware USA. [online] Available from:
679 <https://www.researchgate.net/publication/228492383> (Accessed 5 July 2018), 2006.
- 680 Kundzewicz, Z. W., Mata, L. J., W., A. N., Döll, P., Jimenez, B., Miller, K., Oki, T., Şed, Z. and
681 Shiklomanov, I.: The implications of projected climate change for freshwater resources and their
682 management, *Hydrol. Sci. J.*, 53(1), 3–10, doi:10.1623/hysj.53.1.3, 2008.
- 683 López-Moreno, J. I., Fontaneda, S., Bazo, J., Revuelto, J., Azorin-Molina, C., Valero-Garcés, B.,
684 Morán-Tejeda, E., Vicente-Serrano, S. M., Zubieta, R. and Alejo-Cochachín, J.: Recent glacier
685 retreat and climate trends in Cordillera Huaytapallana, Peru, *Glob. Planet. Change*, 112, 1–11,
686 doi:10.1016/j.gloplacha.2013.10.010, 2014.
- 687 López-Moreno, J. I., Valero-Garcés, B., Mark, B., Condom, T., Revuelto, J., Azorín-Molina, C.,
688 Bazo, J., Frugone, M., Vicente-Serrano, S. M. and Alejo-Cochachin, J.: Hydrological and
689 depositional processes associated with recent glacier recession in Yanamarey catchment,
690 Cordillera Blanca (Peru), *Sci. Total Environ.*, 579, 272–282,
691 doi:10.1016/J.SCITOTENV.2016.11.107, 2017.
- 692 Mark, B. G., French, A., Baraer, M., Carey, M., Bury, J., Young, K. R., Polk, M. H., Wigmore, O.,

- 693 Lagos, P., Crumley, R., McKenzie, J. M. and Lutz, L.: Glacier loss and hydro-social risks in the
694 Peruvian Andes, *Glob. Planet. Change*, 159, 61–76, doi:10.1016/J.GLOPLACHA.2017.10.003,
695 2017.
- 696 Mölg, N., Ceballos, J. L., Huggel, C., Micheletti, N., Rabatel, A. and Zemp, M.: Ten years of
697 monthly mass balance of Conejeras glacier, Colombia, and their evaluation using different
698 interpolation methods, *Geogr. Ann. Ser. A, Phys. Geogr.*, 99(2), 155–176,
699 doi:10.1080/04353676.2017.1297678, 2017.
- 700 Padró, J.-C., Pons, X., Aragonés, D., Díaz-Delgado, R., García, D., Bustamante, J., Pesquer,
701 L., Domingo-Marimon, C., González-Guerrero, Ó., Cristóbal, J., Doktor, D. and Lange, M.:
702 Radiometric Correction of Simultaneously Acquired Landsat-7/Landsat-8 and Sentinel-2A
703 Imagery Using Pseudoinvariant Areas (PIA): Contributing to the Landsat Time Series Legacy,
704 *Remote Sens.*, 9(12), 1319, doi:10.3390/rs9121319, 2017.
- 705 Poveda, G. and Pineda, K.: Reassessment of Colombia's tropical glaciers retreat rates: are they
706 bound to disappear during the 2010–2020 decade?, *Adv. Geosci.*, 22, 107–116,
707 doi:10.5194/adgeo-22-107-2009, 2009.
- 708 Poveda, G., Waylen, P. R. and Pulwarty, R. S.: Annual and inter-annual variability of the
709 present climate in northern South America and southern Mesoamerica, *Palaeogeogr.*
710 *Palaeoclimatol. Palaeoecol.*, 234(1), 3–27, doi:10.1016/j.palaeo.2005.10.031, 2006.
- 711 Rabatel, A., Francou, B., Soruco, A., Gomez, J., Cáceres, B., Ceballos, J. L., Basantes, R.,
712 Vuille, M., Sicart, J.-E., Huggel, C., Scheel, M., Lejeune, Y., Arnaud, Y., Collet, M., Condom, T.,
713 Consoli, G., Favier, V., Jomelli, V., Galarraga, R., Ginot, P., Maisincho, L., Mendoza, J.,
714 Ménégos, M., Ramirez, E., Ribstein, P., Suarez, W., Villacis, M. and Wagnon, P.: Current state
715 of glaciers in the tropical Andes: a multi-century perspective on glacier evolution and climate
716 change, *Cryosph.*, 7(1), 81–102, doi:10.5194/tc-7-81-2013, 2013.
- 717 Rabatel, A., Ceballos, J. L., Micheletti, N., Jordan, E., Braitmeier, M., González, J., Mölg, N.,
718 Ménégos, M., Huggel, C. and Zemp, M.: Toward an imminent extinction of Colombian glaciers?,
719 *Geogr. Ann. Ser. A, Phys. Geogr.*, 1–21, doi:10.1080/04353676.2017.1383015, 2017.
- 720 Ragettli, S., Immerzeel, W. W. and Pellicciotti, F.: Contrasting climate change impact on river
721 flows from high-altitude catchments in the Himalayan and Andes Mountains., *Proc. Natl. Acad.*
722 *Sci. U. S. A.*, 113(33), 9222–7, doi:10.1073/pnas.1606526113, 2016.
- 723 Rekowski, I. C.: Variações de área das geleiras da Colômbia e da Venezuela entre 1985 e
724 2015, com dados de sensoriamento remoto. [online] Available from:
725 <https://www.lume.ufrgs.br/handle/10183/149546> (Accessed 5 July 2018), 2016.
- 726 Ribstein, P., Tiriau, E., Francou, B. and Saravia, R.: Tropical climate and glacier hydrology: a
727 case study in Bolivia, *J. Hydrol.*, 165(1–4), 221–234, doi:10.1016/0022-1694(94)02572-S, 1995.
- 728 Sicart, J. E., Hock, R., Ribstein, P., Litt, M. and Ramirez, E.: Analysis of seasonal variations in
729 mass balance and meltwater discharge of the tropical Zongo Glacier by application of a
730 distributed energy balance model, *J. Geophys. Res.*, 116(D13), D13105,
731 doi:10.1029/2010JD015105, 2011.
- 732 Sorg, A., Bolch, T., Stoffel, M., Solomina, O. and Beniston, M.: Climate change impacts on
733 glaciers and runoff in Tien Shan (Central Asia), *Nat. Clim. Chang.*, 2(10), 725–731,
734 doi:10.1038/nclimate1592, 2012.
- 735 Sorg, A., Huss, M., Rohrer, M. and Stoffel, M.: The days of plenty might soon be over in
736 glacierized Central Asian catchments, *Environ. Res. Lett.*, 9(10), 104018, doi:10.1088/1748-
737 9326/9/10/104018, 2014.
- 738 Soruco, A., Vincent, C., Rabatel, A., Francou, B., Thibert, E., Sicart, J. E. and Condom, T.:
739 Contribution of glacier runoff to water resources of La Paz city, Bolivia (16° S), *Ann. Glaciol.*,
740 56(70), 147–154, doi:10.3189/2015AoG70A001, 2015.
- 741 Stahl, K., Moore, R. D., Shea, J. M., Hutchinson, D. and Cannon, A. J.: Coupled modelling of
742 glacier and streamflow response to future climate scenarios, *Water Resour. Res.*, 44(2),
743 doi:10.1029/2007WR005956, 2008.

744 Stewart, I. T., Cayan, D. R. and Dettinger, M. D.: Changes in Snowmelt Runoff Timing in
745 Western North America under a 'Business as Usual' Climate Change Scenario, *Clim. Change*,
746 62(1–3), 217–232, doi:10.1023/B:CLIM.0000013702.22656.e8, 2004.

747 Vaughan, D. G., Comiso, J. C., Allison, I., Carrasco, J., Kaser, G., Kwok, R., Mote, P., Murray,
748 T., Paul, F., Ren, J., Rignot, E., Solomina, O., Steffen, K. and Zhang, T.: Observations:
749 Cryosphere, in *Climate Change 2013: The Physical Science Basis. Contribution of Working*
750 *Group I to the Fifth Assessment Report of the Intergovernmental Panel on Climate Change*,
751 edited by T. F. Stocker, D. Qin, G.-K. Plattner, M. Tignor, S. K. Allen, J. Boschung, A. Nauels,
752 Y. Xia, V. Bex, and P. M. Midgley, pp. 317–382, Cambridge University Press, Cambridge,
753 United Kingdom and New York, NY, USA., 2013.

754 Vuille, M., Francou, B., Wagnon, P., Juen, I., Kaser, G., Mark, B. G. and Bradley, R. S.: Climate
755 change and tropical Andean glaciers: Past, present and future, *Earth-Science Rev.*, 89(3–4),
756 79–96, doi:10.1016/J.EARSCIREV.2008.04.002, 2008.

757 Vuille, M., Carey, M., Huggel, C., Buytaert, W., Rabatel, A., Jacobsen, D., Soruco, A., Villacis,
758 M., Yarleque, C., Timm, O. E., Condom, T., Salzmann, N. and Sicart, J.-E.: Rapid decline of
759 snow and ice in the tropical Andes – Impacts, uncertainties and challenges ahead, *Earth-*
760 *Science Rev.*, 176, 195–213, doi:10.1016/j.earscirev.2017.09.019, 2017.

761

762

763

764

765

766

767

768

769

770

771

772

773

774

775

776

777

778

779

780

781

782

783

784

785

786

787
788
789
790
791
792
793
794
795
796
797
798
799
800

801 **Table 1.** Hydrologic and climatic indices computed from the hourly streamflow, temperature and
802 precipitation series. * *hpulse* is computed as the hourly equivalent of the melting-runoff spring
803 pulse proposed by Cayan et al. (2001) for daily data, i.e.: the time of the day when the minimum
804 cumulative streamflow anomaly occurs, which is equivalent to finding the hour after which most
805 flows are greater than the daily average.

Index	Explanation	unit
<i>totalQ</i>	total daily water discharge	m ³ day ⁻¹
<i>Qmax</i>	value of maximum hourly water discharge per day	m ³ hour ⁻¹
<i>hpulse*</i>	hour of the day when the melting streamflow pulse starts	hour of the day
<i>Qbase</i>	mean water discharge value between the start of the day (00:00 h) and the hour when <i>hpulse</i> occurs	m ³ hour ⁻¹
<i>hQmax</i>	hour of the day when	hour of the day
<i>Qrange</i>	difference between <i>Qbase</i> and <i>Qmax</i>	m ³ hour ⁻¹
<i>Qslope</i>	slope of the streamflow rising limb between <i>hpulse</i> and <i>hQmax</i>	slope in %
<i>decayslope</i>	slope of the streamflow decaying limb between <i>hQmax</i> and 23:00h	slope in %
<i>Tmax</i>	value of maximum hourly temperature per day	°C hour ⁻¹
<i>Tmin</i>	value of minimum hourly temperature per day	°C hour ⁻¹
<i>Tmean</i>	mean daily temperature	°C day ⁻¹
<i>Trange</i>	difference between <i>Tmin</i> and <i>Tmax</i>	°C hour ⁻¹
<i>hTmax</i>	hour of the day when the <i>Tmax</i> occurs	hour of the day
<i>Diffh</i>	time difference between <i>hTmax</i> and <i>hQmax</i>	Hours
<i>Pmax</i>	value of maximum hourly precipitation per day	mm hour ⁻¹
<i>hPmax</i>	hour of the day when the <i>Pmax</i> occurs	hour of the day
<i>pp</i>	daily precipitation sum	mm day ⁻¹

806
807
808
809
810
811
812
813
814

Table 2. Pearson correlation coefficient between daily hydrological indices and temperature for days with and without precipitation (left) and for days only without precipitation (right) between July 2013 and June 2017. The correlation values correspond to the average obtained by 100 resampling iterations (n = 99) of the correlation test. * and ** indicate that correlations are significant at 95% and 99% confidence respectively (two-tailed test).

Index	days with and without precipitation (n = 99)				days without precipitation (n = 99)			
	<i>Tmin</i>	<i>Tmax</i>	<i>Tmean</i>	<i>Trange</i>	<i>Tmin</i>	<i>Tmax</i>	<i>Tmean</i>	<i>Trange</i>
<i>total</i>	0.25**	0.12	0.19	0.02	0.31**	0.54**	0.53**	-0.39**
<i>Qmax</i>	0.25**	0.30**	0.33**	-0.18	0.24*	0.64**	0.57**	-0.54**
<i>Qbase</i>	0.13	-0.13	-0.05	0.22*	0.18	0.05	0.11	0.06
<i>Qrange</i>	0.25**	0.36**	0.37**	-0.25**	0.22*	0.65**	0.58**	-0.57**
<i>Qslope</i>	0.18	0.40**	0.38**	-0.34**	0.12	0.58**	0.48**	-0.55**
<i>hQmax</i>	0.06	-0.03	0.00	0.06	0.04	0.00	0.02	0.02
<i>Hpulse</i>	-0.18	-0.17	-0.21*	0.08	-0.36**	-0.50**	-0.52**	0.31**

815

816

817 **Table 3.** Mean and standard deviation of variance explained (%) by each PC throughout the 25
818 bootstrapped samples

PC	Mean	standard deviation
PC1	47.78	5.91
PC2	34.99	5.66
PC3	11.82	6.77

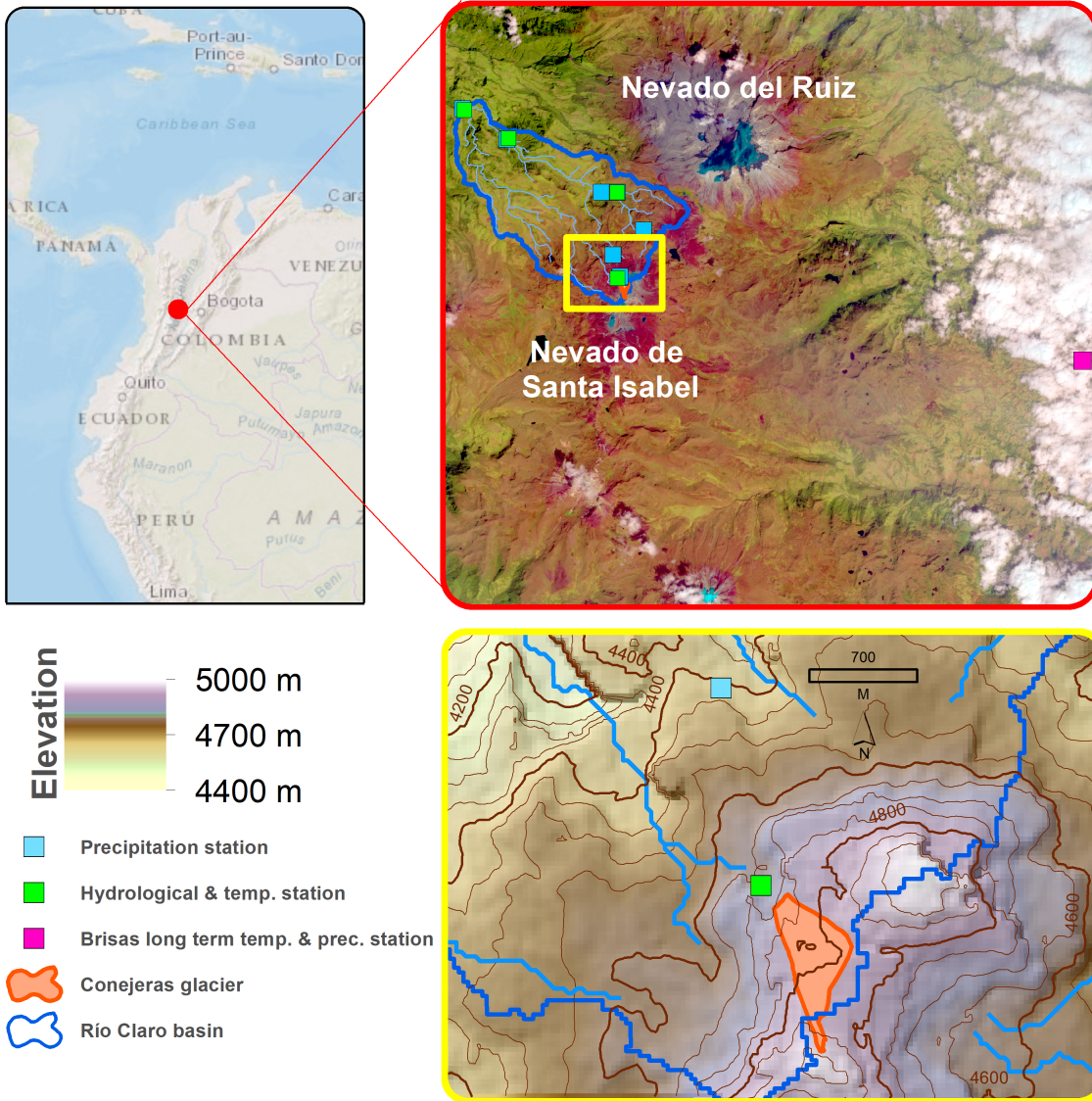
819

820

821

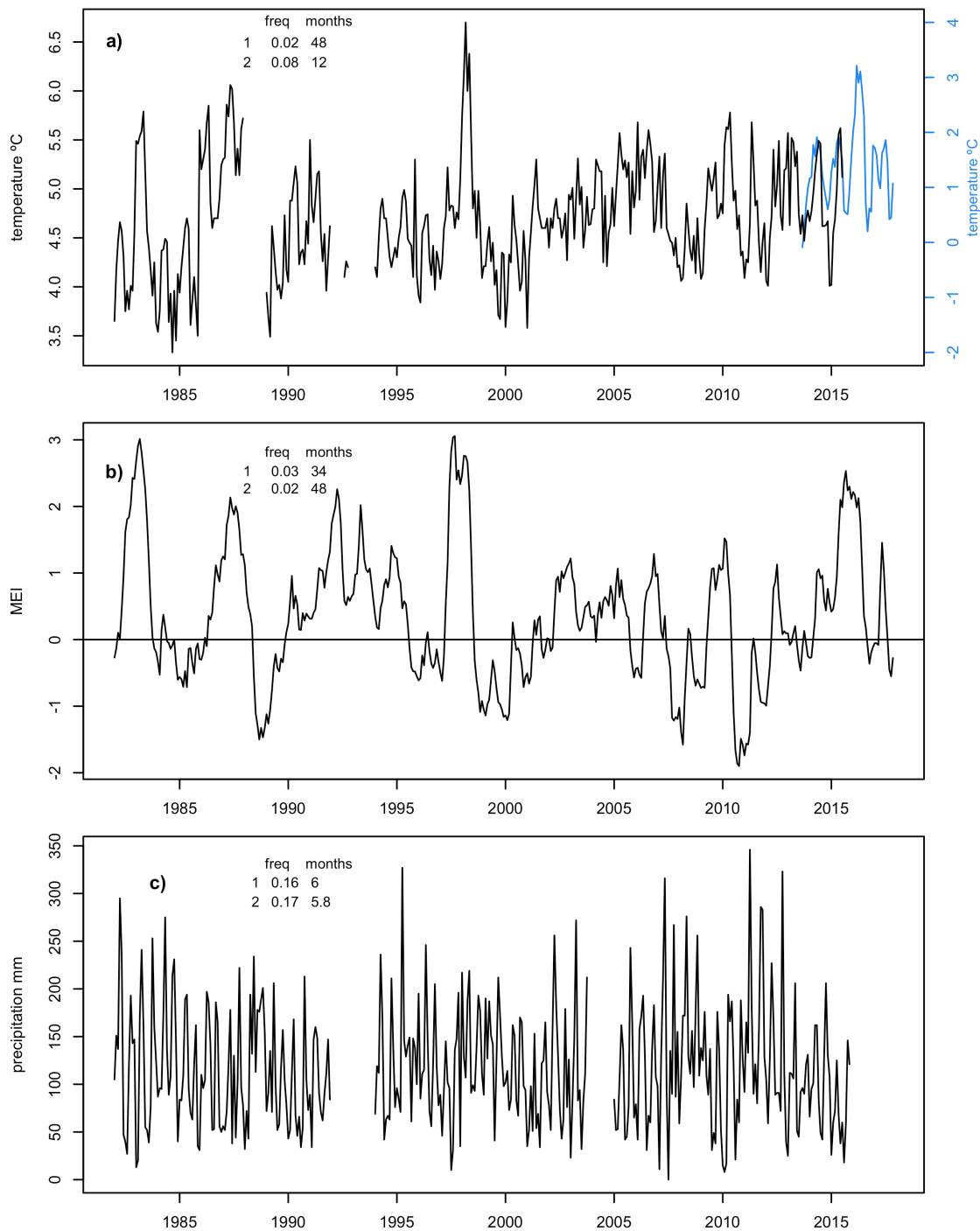
822

823



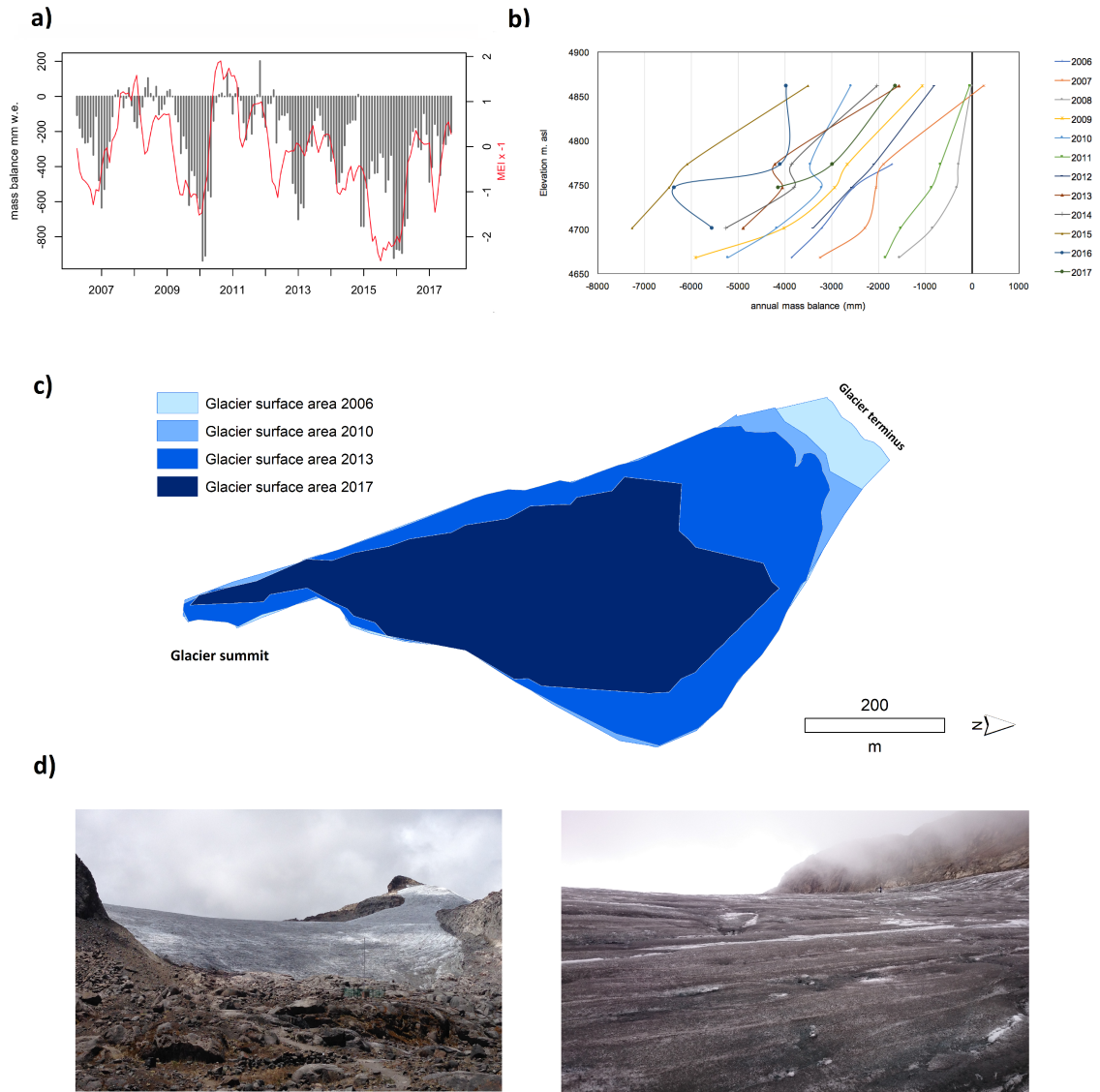
824
825
826
827

Figure 1. Study area, showing the glaciers of the Parque Nacional Natural de los Nevados, and the Río Claro river basin (top map) and the Conejeras glacier with hydro-meteorological stations (bottom map).



828

829 **Figure 2.** Long-term evolution of climate variables in the study area. a) monthly air temperature
 830 at the Brisas meteorological station (2721 m. asl), 1982-2015 (black line), and the temperature at
 831 the glacier snout (note the difference in the range of values), 2013-2017 (blue line); b) Multivariate
 832 ENSO Index; c) monthly precipitation at the Brisas station, 1982-2015; The frequency and its
 833 equivalent in months (1/frequency) of the two top spectral densities from spectral analysis is
 834 shown for temperature, MEI and precipitation monthly series.



835

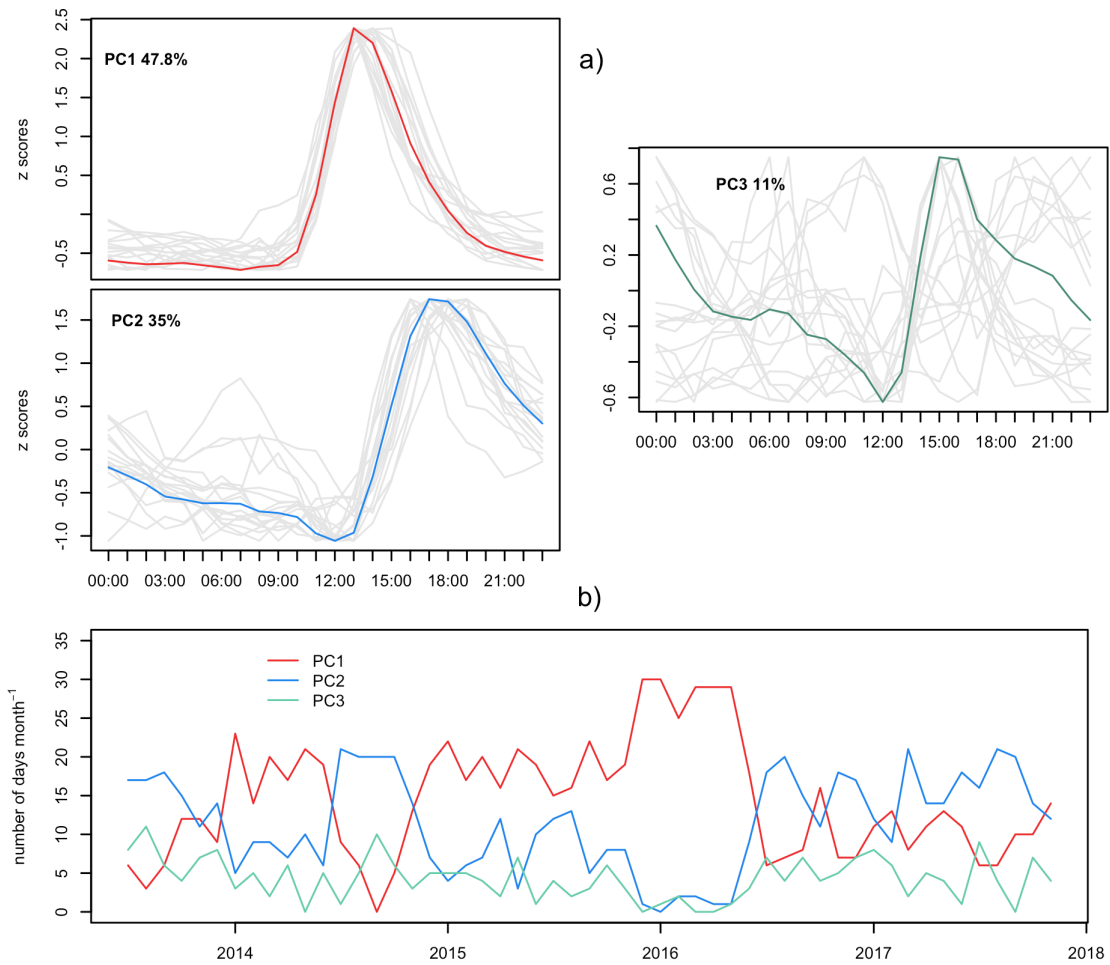
836 **Figure 3.** Evolution of the Conejeras glacier. a) monthly mass balance in mm w.e. and Multivariate
 837 ENSO Index (not the inverted axis). b) annual mass balance per altitudinal range. c) extension of
 838 the glacier in hectares in 2006, 2010, 2013 and 2017. d) Photographs of the glacier surface
 839 covered by volcanic ashes, taken in 2015 and 2016.

840

841

842

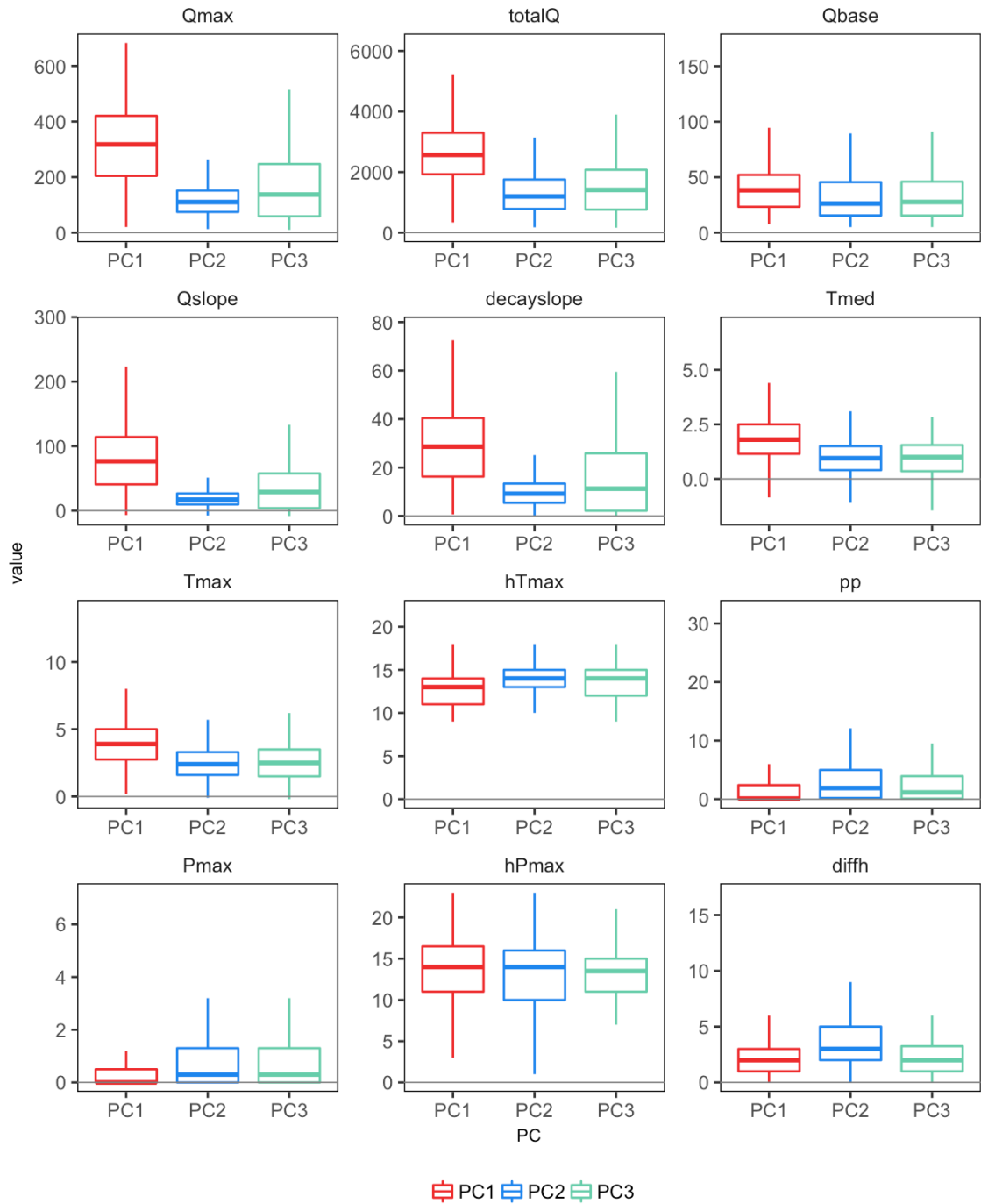
843



844

845

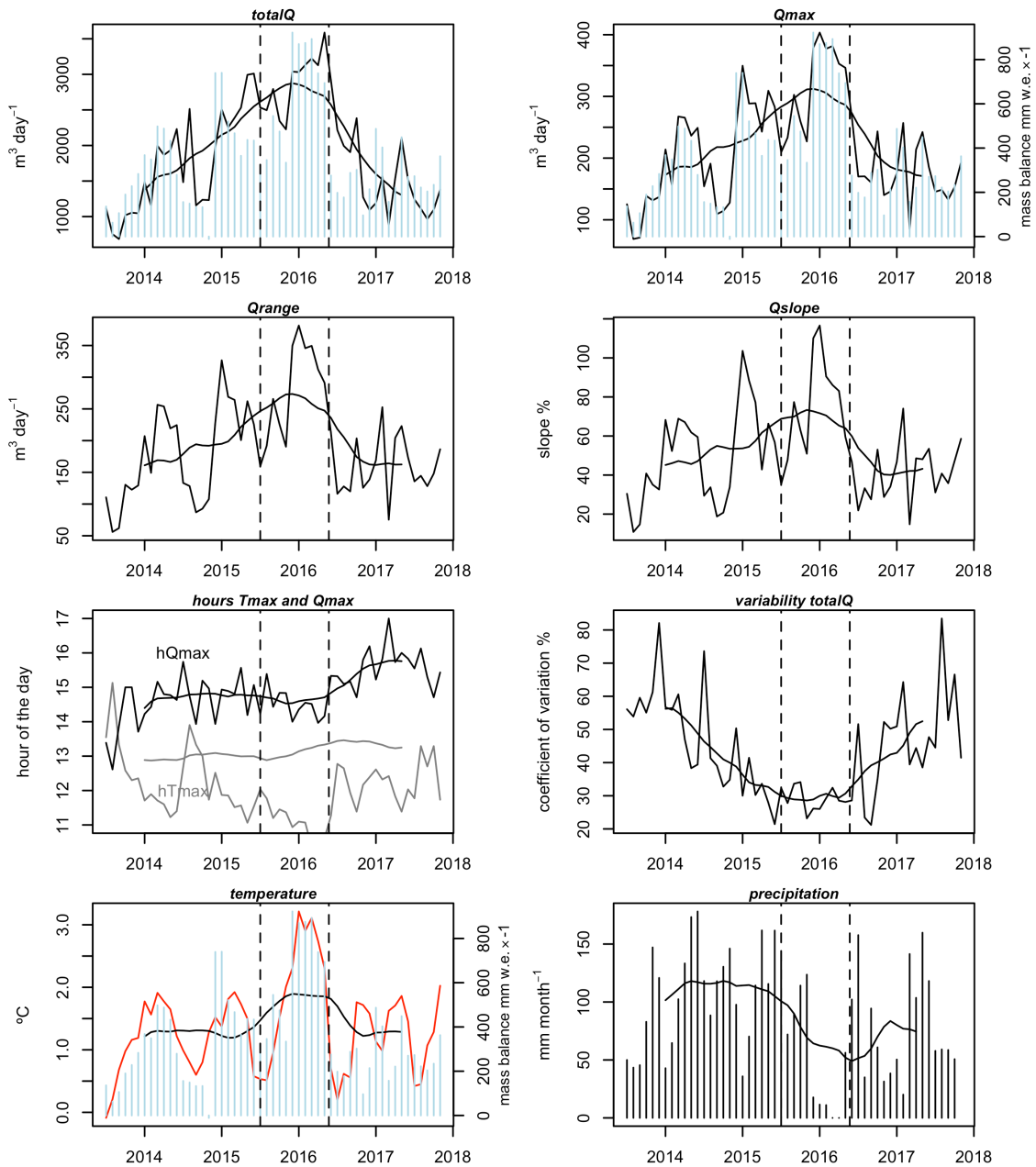
846 **Figure 4.** Principal Component Analysis on hourly streamflow. a) scores of the three main
 847 principal components (patterns of daily streamflow), with gray lines indicating the scores for each
 848 one of the 25 bootstrapped samples in the recursive PCA, and colored lines indicating the
 849 average. b) Evolution of the number of days per month that show maximum correlation with each
 850 PC. Red corresponds to PC1, blue corresponds to PC2 and green corresponds to PC3



851

852 **Figure 5.** Summary of the frequency distributions (boxplots) of the hydrological and
 853 meteorological indicators for days grouped within PC1, PC2 and PC3.

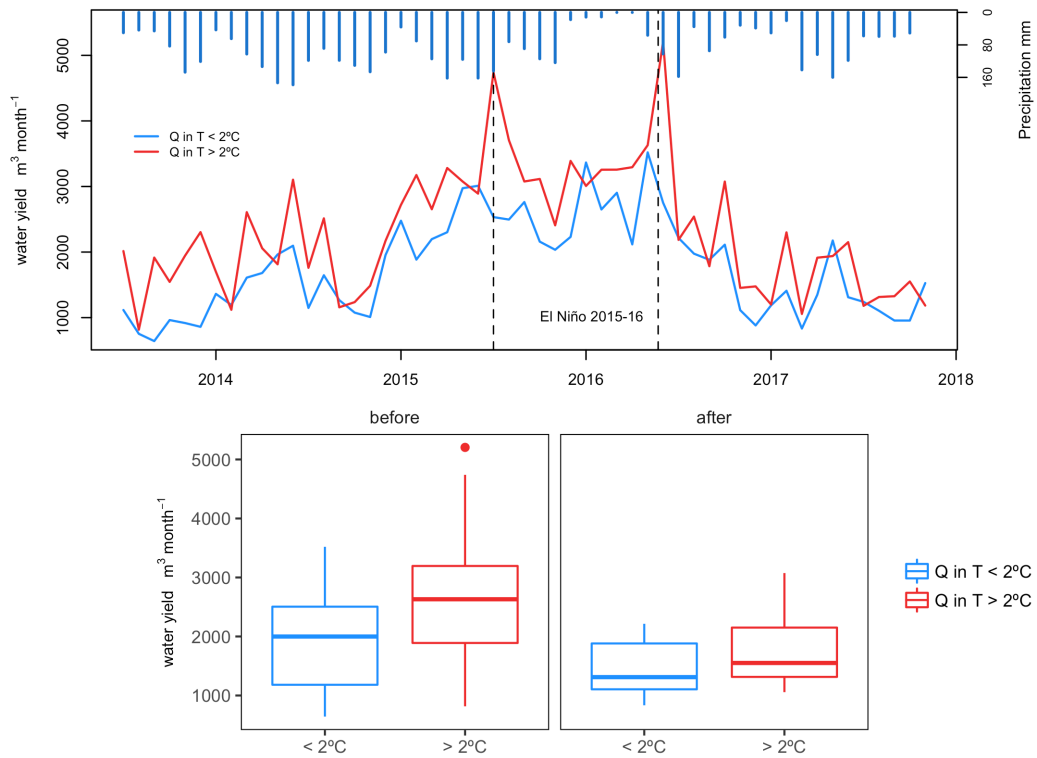
854



855

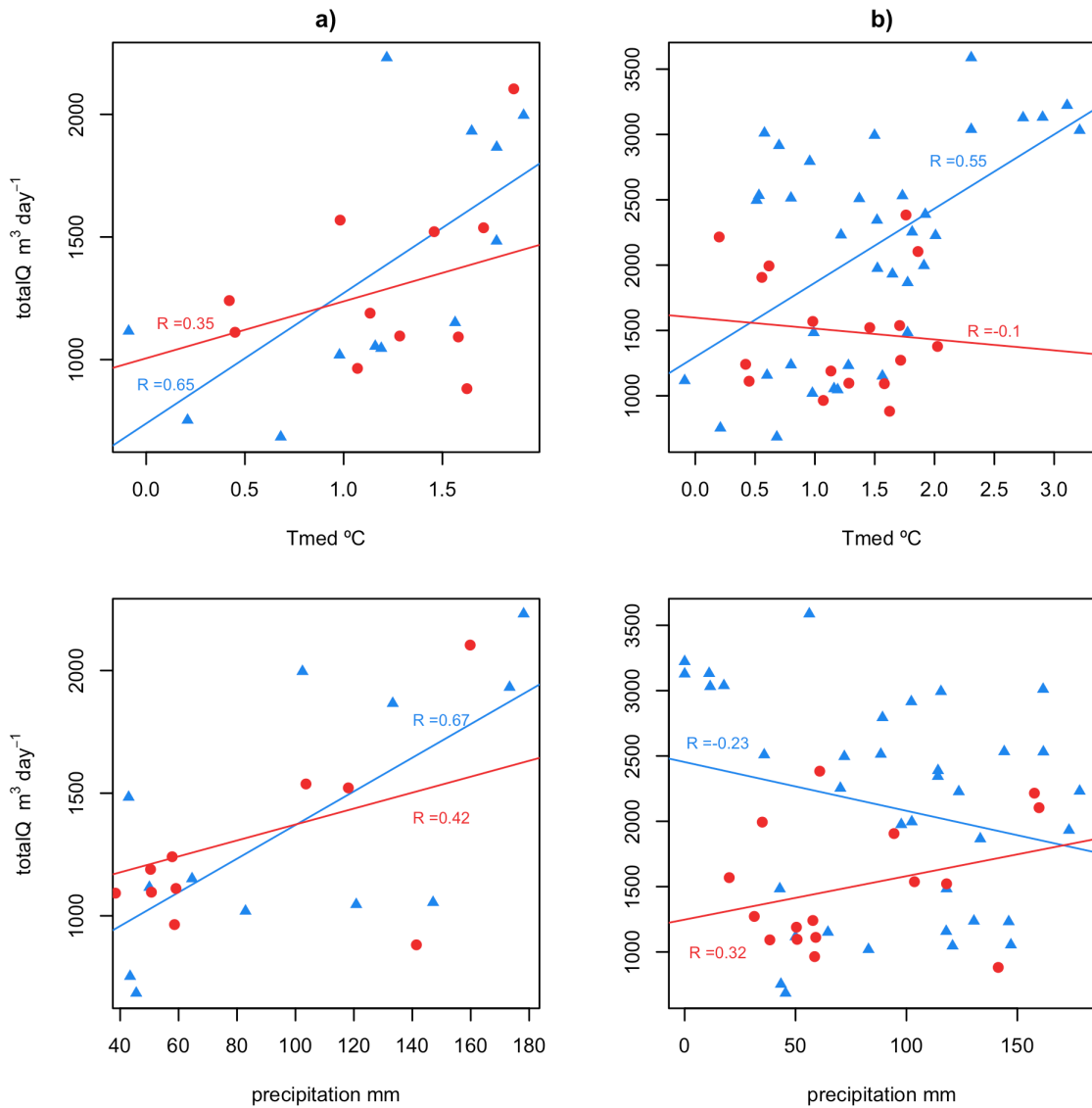
856 **Figure 6.** Evolution of monthly averaged hydrological indices, temperature, precipitation and
 857 glacier mass balance (in blue bars), for the study period. Dashed lines indicate the 2015-2016
 858 strong El Niño event. 12-months window moving average (black smooth lines) are shown to
 859 represent trends.

860



861

862 **Figure 7.** Mean monthly water discharge (Q), for days with temperature lower than 2°C (blue)
 863 and days with temperature higher than 2°C (red) Top: Inter-annual evolution with indication of El
 864 Niño 2015-16 event (grey shading), breakpoint in water discharge evolution (dashed line), and
 865 monthly precipitation (blue bars); bottom: comparative boxplots for water discharge before and
 866 after breakpoint in May 2016.



867

868 **Figure 8.** Correlations between monthly flow and monthly temperature (top plots) and
 869 precipitation (bottom plots) for: a) 2013-14 (blue triangles) and 2017 (red circles) years, which are
 870 considered as analogues in terms of amounts of flow; and b) months before May 2016 breakpoint
 871 (blue triangles) and months after May 2016 breakpoint (red circles).

872